基于柔性的高酞酸和双咪唑型配体的 Ni(Ⅱ)/Cd(Ⅱ)/Zn(Ⅱ)配位聚合物的合成、结构和性质

鞠丰阳[1] 李云平[2] 刘广臻*,[2]
([1]洛阳师范学院食品与药品学院,洛阳 471934)
([2]洛阳师范学院化学化工学院,河南省功能导向多孔材料重点实验室,洛阳 471934)

摘要:基于柔性的高酞酸(H_2hmph)和双咪唑型配体,通过溶剂热法合成了 3 种新的配位聚合物:{[Ni_2(hmph)$_2$(bib)$_2$(H_2O)$_2$]·3H_2O}$_n$ (**1**)、[Cd(hmph)(bib)]$_n$ (**2**)和{[Zn(hmph)(bip)]·H_2O}$_n$ (**3**),其中 bib=1,4-双(1-咪唑基)苯、bip=3,5-双(1-咪唑基)吡啶。配合物 **1** 是由 Ni-羧酸链之间通过 bib 配体桥联而成的二维单层结构;配合物 **2** 为 Cd-羧酸双股链之间通过 bib 配体拓展而成的二维双层结构,并含有由羧基连接的双核单元;配合物 **3** 是由羧酸连接而成的双核 Zn 单元通过 bip 配体拓展形成的双股链。3 个配合物都具有较高的热稳定性。磁性分析表明在配合物 **1** 中存在铁磁性交换偶合作用。另外,配合物 **2** 和 **3** 的荧光性质与相应的配体相比都表现出明显的蓝移。

关键词:高酞酸;双咪唑型;配位聚合物;磁性质;荧光性质
中图分类号:O614.81$^+$3;O614.24$^+$2;O614.24$^+$1 **文献标识码**:A **文章编号**:1001-4861(2020)02-0368-09
DOI:10.11862/CJIC.2020.044

Syntheses, Structures and Properties of Ni(Ⅱ)/Cd(Ⅱ)/Zn(Ⅱ) Complexes with Flexible Homophthalic Acid and Diimidazolyl-Type Ligands

JU Feng-Yang[1] LI Yun-Ping[2] LIU Guang-Zhen*,[2]
([1]*School of Food and Drug, Luoyang Normal University, Luoyang, Henan* 471934, *China*)
([2]*College of Chemistry and Chemical Engineering, Henan Key Laboratory of Function-Oriented Porous Materials, Luoyang Normal University, Luoyang, Henan* 471934, *China*)

Abstract: Based on flexible homophthalic acid (H_2hmph) and diimidazolyl-type ligands, three novel coordination polymers with the formulas determined as {[Ni_2(hmph)$_2$(bib)$_2$(H_2O)$_2$]·3H_2O}$_n$ (**1**), [Cd(hmph)(bib)]$_n$ (**2**) and {[Zn(hmph)(bip)]·H_2O}$_n$ (**3**) (bib=1,4-bis(1-imidazolyl)benzene; bip=3,5-bis(1-imidazolyl)pyridine) have been solvothermally synthesized. Complex **1** displays a 2D mono-layer structure featuring Ni-carboxylate chains cross-linked further by bib co-ligands. Complex **2** exhibits a 2D bilayer structure containing double-stranded Cd-carboxylate chains bridged by bib co-ligands, wherein there are carboxyl-bridged dinuclear kernels. Complex **3** is double-stranded chain featuring Zn-carboxylate binuclear units extended further by bip co-ligands. TGA experiments show that all three complexes have high thermal stabilities. And the magetic data indicate there is typical ferromagnetic exchange coupling in complex **1**. Furthermore, the fluorescent properties of both complexes **2** and **3** show significant blue-shift compared with the free ligands. CCDC: 1935595, **1**; 1935596, **2**; 1935599, **3**.

Keywords: homophthalic acid; diimidazolyl; coordination polymers; magnetic property; fluorescent property

收稿日期:2019-07-02。收修改稿日期:2019-11-04。
国家自然科学基金(No.21571093)资助项目。
*通信联系人。E-mail:gzliuly@126.com

Coordination polymers (CPs) are crystalline materials constructed by conformationally rigid or flexible organic ligands with different inorganic metal centers[1-3]. Typically, the self-assembly process of CPs is controllable to achieve targeting CPs with intriguing topologies, high thermal stabilities and desirable attributes through rational design of rigid organic components[4-5]. So, rigid ligands with aromatic multi-carboxyl, pyridyl or imidazolyl moieties are employed widely, yielding prolific production of CPs[6-10]. And the self-assembly process becomes challengeable when the flexible organic components are used[11-12]. As we all known, molecular flexibility is derived from the sp^3-hybridized carbon atom, allowing rotation about C-C single bond and different conformational preference[13]. In terms of CPs, the ultimate conformations of flexible ligands are sensitive to many factors, such as the versatile coordination geometries of metal ions, co-existing substituent groups, auxiliary rigid ligands, counter ions, pH value and temperature[14-17]. Indeed, it has been demonstrated that conformational freedom may provide rare opportunities to generate CPs with structural diversity which is inaccessible from rigid ligands, chiral centers and dynamic behavior[18-21].

Particularly, others and our team have endeavored to the investigations of CPs assembled from homophthalic acid (H_2hmph)[22-30]. As an asymmetric flexible ligand possessing both rigid -COOH group and flexible -CH_2COOH group, homophthalic acid has been used to construct CPs with structures from discrete, 1D chain, 2D lamella, 2D thick-layer, 3D microporous framework to 3D→3D self-penetrated net. And these limited studies have proven that homophthalic acid is an efficient flexible ligand, which can provide strong coordination capability and versatile coordination modes. To broaden our knowledge of the coordination chemistry of homophthalic acid ligand, 1,4-bis(1-imidazolyl)benzene (bib) and 3,5-bis(1-imidazolyl)pyridine (bip) were introduced into the assembled systems of CPs. As novel diimidazolyl-type ligands, two imidazolyl rings in their structures are spaced by phenyl ring and pyridiyl ring, respectively. Additionally, the places of imidazolyl rings attached to phenyl ring and pyridiyl ring are different from each other. Distinct electronic cloud densities and spatial effects can influence the structures and properties of the resulted CPs.

In this work, we obtained three coordination polymers, namely $\{[Ni_2(hmph)_2(bib)_2(H_2O)_2]\cdot 3H_2O\}_n$ (**1**), $[Cd(hmph)(bib)]_n$ (**2**) and $\{[Zn(hmph)(bip)]\cdot H_2O\}_n$ (**3**). And the preparations, crystal structures, thermal stabilities, magnetic property for complex **1** and fluorescent properties for **2** and **3** are described as below.

1 Experimental

1.1 Materials and methods

All chemical reagents were purchased from reagent companies and used directly without any purification. Elemental analyses (C, H and N) were performed on a Flash EA 2000 elemental analyzer. Infrared spectra (IR) were measured by a Nicolet 6700 FT-IR spectrophotometer. The powder X-ray diffraction determinations (PXRD) were recorded by using a Bruker AXS D8 Advance diffractometer with monochromated Cu $K\alpha$ radiation (λ=0.154 18 nm; generator current: 40 mA; generator voltage: 40 kV; scanning range: 5°~50°). The thermogravimetric analysis experiments (TGA) were carried out on a SII EXStar6000 TG/DTA6300 analyzer at a heating rate of 10 ℃·min^{-1} under N_2 atmosphere. Variable-temperature magnetic susceptibility measurement was performed on a Quantum Design SQUID MPMS XL-7 instrument from 2.5 to 300 K under an applied magnetic field of 2 000 Oe. Luminescence spectra were performed on a Hitachi F-7000 spectrophotometer at room temperature.

1.2 Preparation of the complexes

All three complexes were realized through facile solvothermal method. Starting materials were placed in a 7 mL penicillin bottle and sealed in 23 mL PTFE-lined stainless steel autoclave. The reactor was heated to given temperature (120 ℃ for **1** and **2**, 160 ℃ for 3) under autogenous pressure for 3 days and then cooled naturally to room temperature. The crystals were dried and collected after they were washed with distilled water and ethanol. The phase purities of all

three complexes were confirmed by PXRD measurements at room temperature. Each PXRD pattern of the as-synthesized sample agrees well with the simulated one based on the structure solutions, indicative of the purity of the bulk sample (Supporting information, Fig. S1, S2 and S3).

Synthesis of $\{[Ni_2(hmph)_2(bib)_2(H_2O)_2]\cdot 3H_2O\}_n$ (**1**): In the presence of aqueous NaOH solution (0.5 mol·L^{-1}, 0.1 mL), the mixture of homophthalic acid (0.1 mmol, 18.0 mg), 1,4-bis(1-imidazolyl)benzene (0.1 mmol, 21.0 mg), $Ni(OAc)_2\cdot 4H_2O$ (0.2 mmol, 49.8 mg) was suspended in distilled water (6.0 mL), giving green sheet crystals after solvothermal reaction (56% based on Ni). Anal. Calcd. for $C_{42}H_{42}Ni_2N_8O_{13}$(%): C, 51.25; H, 4.30; N, 11.39. Found(%): C, 51.22; H, 4.36; N, 11.34. IR (cm^{-1}): 3 427(w), 3 130(w), 1 551(s), 1 521(s), 1 379 (s), 1 303(m), 1 228(w), 1 062(s), 960(m), 934(m), 863 (w), 829(m), 814(m), 728(s), 651(s).

Synthesis of $[Cd(hmph)(bib)]_n$ (**2**). In the presence of aqueous HAc solution (0.5 mol·L^{-1}, 0.2 mL), the mixture of homophthalic acid (0.1 mmol, 18.0 mg), 1,4-bis(1-imidazolyl)benzene (0.2 mmol, 42.0 mg), $Cd(OAc)_2\cdot 2H_2O$ (0.2 mmol, 53.3 mg) and H_2O (6.0 mL) gave colourless blocked crystals after solvothermal reaction (72% based on Cd). Anal. Calcd. for $C_{21}H_{16}CdN_4O_4$(%): C, 50.37; H, 3.22; N, 11.19. Found(%): C, 50.32; H, 3.25; N, 11.27. IR (cm^{-1}): 3 119(w), 1 576(s), 1 524(s), 1 490(m), 1 384(s), 1 302(s), 1 271(m), 1 133(s), 1 103 (s), 1 065(s), 1 051(s), 955(s), 928(m), 839(s), 821(s), 732(s), 701(m), 667(s).

Synthesis of $\{[Zn(hmph)(bip)]\cdot H_2O\}_n$ (**3**). The mixture of homophthalic acid (0.1 mmol, 18.0 mg), 3,5-bis(1-imidazolyl)pyridine (0.2 mmol, 42.0 mg), $Zn(OAc)_2\cdot 2H_2O$ (0.2 mmol, 43.9 mg) was suspended in H_2O-methanol solution (6 mL, 2∶1, *V*/*V*), giving colourless blocked crystals after solvothermal reaction (54% based on Zn). Anal. Calcd. for $C_{20}H_{17}ZnN_5O_5$(%): C, 50.81; H, 3.62; N, 14.81. Found (%): C, 50.77; H, 3.65; N, 14.76. IR (cm^{-1}): 3 441(w), 3 128(w), 1 634(s), 1 585(s), 1 559(s), 1 503(s), 1 383(s), 1 361(s), 1 312 (m), 1 256(s), 1 110(s), 1 061(s), 1 005(m), 956(m), 941(m), 878(s), 840(s), 728(s), 691(s), 646(s).

1.3 X-ray crystallography

Single-crystal X-ray diffraction data for complexes **1**~**3** were collected on a Bruker SMART APEX Ⅱ CCD diffractometer equipped with graphite-monochromated Mo $K\alpha$ radiation (λ=0.071 073 nm). Using Olex2 software, all three structures were solved by direct method and refined with SHElXL-2015 refinement package by least squares minimisation[31-33]. Hydrogen atoms were fixed at their calculated positions with the riding model. The U_{iso} values for H atoms of organic ligands were 1.2 times U_{eq} of their attached carbon atoms, and they were 1.5 times U_{eq} of their attached oxygen atoms for the hydrogen atoms at water. The details of the structure solution and final refinements are listed in Table 1.

CCDC: 1935595, **1**; 1935596, **2**; 1935599, **3**.

Table 1 Crystal and structure refinement data for complexes 1~3

	1	2	3
Empirical formula	$C_{42}H_{42}Ni_2N_8O_{13}$	$C_{21}H_{16}CdN_4O_4$	$C_{20}H_{17}ZnN_5O_5$
Formula weight	984.25	500.78	472.76
Crystal system	Monoclinic	Triclinic	Triclinic
Space group	$P2_1/n$	$P\bar{1}$	$P\bar{1}$
a / nm	1.328 32(11)	0.787 9(6)	0.893 56(5)
b / nm	0.902 68(7)	0.991 7(7)	1.046 85(6)
c / nm	1.810 85(15)	1.326 1(9)	1.121 85(6)
α / (°)		73.638(15)	67.482 0(10)
β / (°)	105.115(2)	78.862(17)	81.466 0(10)
γ / (°)		73.637(15)	73.942 0(10)
V / nm^3	2.096 2(3)	0.946 6(12)	0.930 51(9)
Z	2	2	2

Continued Table 1

D_c / (g·cm^{-3})	1.559	1.757	1.687
μ / mm^{-1}	0.976	1.192	1.367
F(000)	1 020	500	484
θ range / (°)	3.414~50.122	3.226~50.602	3.934~51
Reflection collected, unique	13 126, 3 711	6 178, 3 396	6 257, 3 452
R_{int}	0.041 6	0.020 0	0.013 8
Completeness to θ / %	99.9	98.9	99.7
Data, restraint, parameter	3 711, 12, 298	3 396, 0, 271	3 452, 0, 280
Goodness-of-fit	1.038	1.061	1.056
R_1	0.035 9	0.020 7	0.023 2
wR_2 [I>2σ(I)]	0.087 0	0.051 1	0.061 0
R_1 (all data)	0.047 1	0.022 7	0.024 7
wR_2 (all data)	0.094 1	0.053 2	0.061 9
$(\Delta\rho)_{max}$ and $(\Delta\rho)_{min}$ / (e·nm^{-3})	410, −530	360, −330	260, −360

2　Results and discussion

2.1　Crystal structure

2.1.1　Structural description of {[Ni_2(hmph)$_2$(bib)$_2$(H_2O)$_2$]·3H_2O}$_n$ (**1**)

Complex **1** belongs to the monoclinic crystal system of $P2_1/n$ space group. The asymmetric unit consists of one Ni(Ⅱ) cation, one completely deprotonated hmph^{2-} dianion, one bib molecule, one coordinating water molecule and one and a half guest water molecules, as shown in Fig.1a. The unique Ni atom displays a [NiO_4N_2] octahedral geometry with the coordination sphere defined by three oxygen atoms from two symmetry related hmph^{2-} moieties, the last one oxygen atom from one coordinating water and two N atoms from two bib. The Ni-O bond lengths range from 0.206 17(19) to 0.209 57(17) nm, while the Ni-N bond lengths are 0.206 3(2) and 0.207 5(2) nm. The

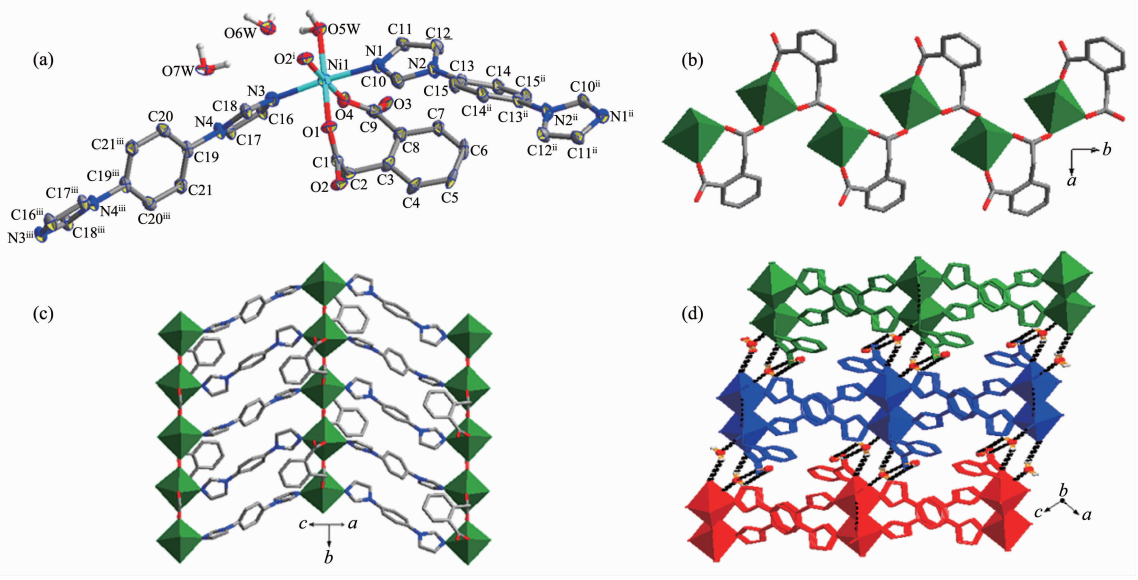

Symmetry codes: [i] −x+1/2, y−1/2, −z+1/2; [ii] −x, −y+2, −z+1; [iii] −x+1, −y+2, z; Displacement ellipsoids are drawn at the 50% probability level and all hydrogen atoms of carbon atoms are omitted for clarity

Fig.1　(a) View of coordination environment of Ni(Ⅱ) in complex **1**; (b) View of Ni-carboxylate chain spaced by carboxylate ligands; (c) View of monolayer structure lying in bc plane; (d) 3D supramolecular structure fabricated by H-bonding interactions labeled as dark dotted lines

$[NiO_4N_2]$ units are connected by the flexible $-CH_2COO^-$ groups in bridging bidentate mode to form a metal-carboxylate chain with the intrachain Ni…Ni separation of 0.533 83(5) nm, wherein the O-C-C-C-C-C-O-Ni eight-membered rings are fabricated by the cooperation of the rigid $-COO^-$ groups in monodentate mode and the $-CH_2COO^-$ groups (Fig.1b). And the 1D motifs are further bridged by the bib molecules along *c* direction to generate an irregular metal-organic monolayer paralleling to *bc* plane, in which the Ni…Ni separations are 1.361 95(9) nm and 1.356 28(10) nm (Fig.1c). This monolayer employs the mentioned eight-membered rings acting as pendent arms above and below. Moreover, the adjacent bib bridges are of certain angle and every other bib bridges are parallel, probably because of the spatial effect resulting from the eight-membered rings. Particularly, the presence of coordinated and free water molecules leads to the formation of abundant H-bonding interactions. Through the cooperations of O(5W)–H(5WB)…O(6W) (O…O 0.280 3(3) nm, ∠O–H…O=173.1°) with O(6W)–H(6WA)…O(4)^{iii} (O…O 0.326 0(4) nm, ∠O–H…O=150.8°), O(6W)–H(6WB…O(3)^{iii} (O…O 0.282 3(4) nm, ∠O–H…O=128.2°), O(7W)–H(7WA)…O(6W) (O…O 0.298 3(8) nm, ∠O–H…O=152.6°) and O(7W)–H(7WB) …O(3)^{iii} (O…O 0.278 2(7) nm, ∠O–H…O=159.3°), individual layers are stacked to create the whole 3D supramolecular structure (Fig.1d).

2.1.2 Structural description of $[Cd(hmph)(bib)]_n$ (**2**)

Complex **2** crystallizes in the triclinic crystal system of $P\bar{1}$ space group. The asymmetric unit is comprised of one Cd (Ⅱ) cation, one completely deprotonated $hmph^{2-}$ dianion and one bib molecule, as shown in Fig.2a. The center Cd ion displays a $[CdO_4N_2]$ octahedral geometry with the coordination sphere defined by four oxygen atoms from three symmetry related $hmph^{2-}$ dianions, and two terminal N atoms from two bib molecules. All Cd-O bond lengths fall in a range from 0.224 9(2) to 0.277 39(14) nm, while the Cd-N bond lengths are 0.228 0(2) and 0.230 2(2) nm. Two Cd octahedra are double bridged by two $-CH_2COO^-$ groups to form one dinuclear kernel with the Cd…Cd separation of 0.398 31(21) nm (Fig. 2b). These adjacent dinuclear units are further connected to generate a double-stranded chain along a direction through μ_2-$hmph^{2-}$ dianion with $-COO^-$ groups in chelating coordination mode and $-CH_2COO^-$ groups in bridging bidentate mode. And in such manner, an alternating arrangement of 8-membered and 16-membered metal-organic ring is fabricated. Furthermore, the 1D chains are bridged by μ_2-bib ligands to produce a 2D bilayer (Fig.2c). Individual layers are stacked to create the ultimate 3D supramolecular structure by weak van der Waals forces since there are only intralayer π-π stacking interactions between the phenyl rings of bib molecules with

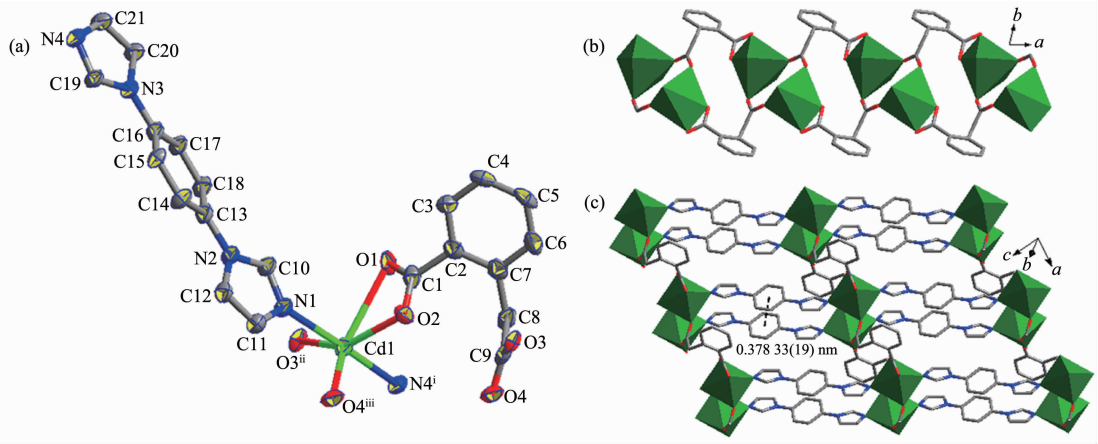

Symmetry codes: ^{i} $x-1, y, z+1$; ^{ii} $x+1, y, z$; ^{iii} $-x+1, -y+1, -z+1$; Displacement ellipsoids are drawn at the 50% probability level and all hydrogen atoms of carbon atoms are omitted for clarity

Fig.2 (a) View of coordination environment of Cd(Ⅱ) in complex **2**; (b) View of Cd-carboxylate chain containing an alternating arrangement of 8-membered and 16-membered rings; (c) View of 2D bilayer with intralayer π-π interactions

the centroid-centroid distances of 0.378 33(19) nm.

2.1.3 Structural description of $\{[Zn(hmph)(bip)]\cdot H_2O\}_n$ (**3**)

Complex **3** also crystallizes in the triclinic crystal system of $P\bar{1}$ space group. The asymmetric unit comprises one Zn(Ⅱ) cation, one completely deprotonated $hmph^{2-}$ dianion, one bip molecule and one uncoordinated water molecule, as shown in Fig.3a. The centre Zn ion exhibits a $[ZnN_2O_2]$ tetrahedral geometry with the coordination sphere defined by two oxygen atoms from two symmetry related $hmph^{2-}$ dianions, and two N atoms from two bip molecules. The Zn-O bond lengths are 0.194 06(13) and 0.194 72(12) nm. The Zn-N bond lengths are 0.200 76(14) and 0.204 89(14) nm. Two neighbor tetrahedra are double bridged by two μ_2-$hmph^{2-}$ dianions adopting monodentate mode to form one dinuclear unit with the Zn…Zn separation of 0.537 52(2) nm (Fig.3b). Meanwhile, one 16-membered metal-organic ring is observed. The ancillary μ_2-bip ligand molecules link adjacent dinuclear units to form a double-stranded chain structure. Individual chains are propagated to 2D layer structure through only two kinds of H-bonds originating from the uncoordinated water molecules and organic ligands (Fig.3c). Moreover, there are obvious intralayer π-π stacking interactions between the pyridine rings of bip molecules with the centroid-centroid distances of 0.390 97(2) nm (Fig.3d). So, the ultimate 3D supramolecular structure of complex **3** is maintained by weak van der Waals forces only.

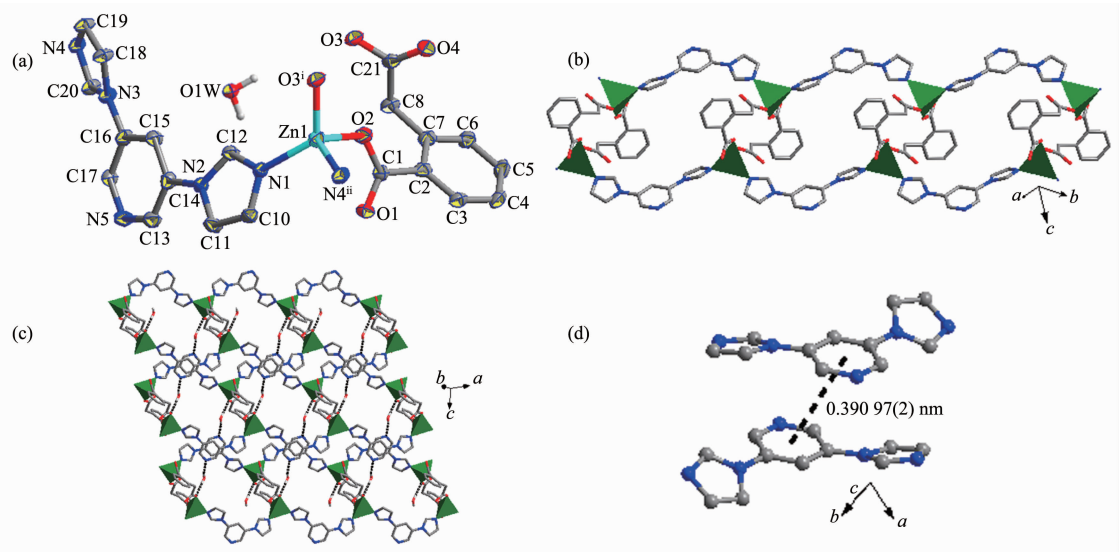

Symmetry codes: i −*x*+2, −*y*+2, −*z*; ii *x*+1, *y*−1, *z*; Displacement ellipsoids are drawn at the 50% probability level and all hydrogen atoms of carbon atoms are omitted for clarity

Fig.3 (a) View of coordination environment of Zn(Ⅱ) in complex **3**; (b) View of Zn-organic chain based on dinuclear units containing 16-membered rings; (c) View of 2D layer structure propagated through only two kinds of H-bonds labeled as dark dotted lines; (d) Intralayer π-π stacking interaction between the pyridine rings of bip molecules

2.2 Thermogravimetric analyses

TGA experiments for complexes **1**~**3** were carried out to monitoring their thermal stability, as shown in Fig.4. For complex **1**, the TGA curve illustrated one distinct weight loss from 160 to 197 ℃, equivalent to two and a half water molecules (Calcd. 9.14%, Obsd. 8.70%). And the succeeding weight-loss between 267 and 402 ℃ can be assigned to the decomposition of organic components. The final residue is attributed to NiO phase (Calcd. 15.18%, Obsd. 16.29%). Complex **2** can survive before 304 ℃ and then decomposed with a two-step weight loss until 515 ℃. The residue weighing 25.49% of the total sample corresponds to the CdO component (Calcd. 25.64 %). The TGA curve of complex **3** showed the removal of one guest water molecule from 155 to 227 ℃ with a slight weight loss (Calcd. 3.81%, Obsd. 3.59%). And two sharp weight-loss processes were obseved within a range of 292 to

545 ℃, which are attributed to the collapse of the framework. The remnant holding a weight of 25.37% may be the mixture of ZnO (Calcd. 17.21%) and unburned carbon[34].

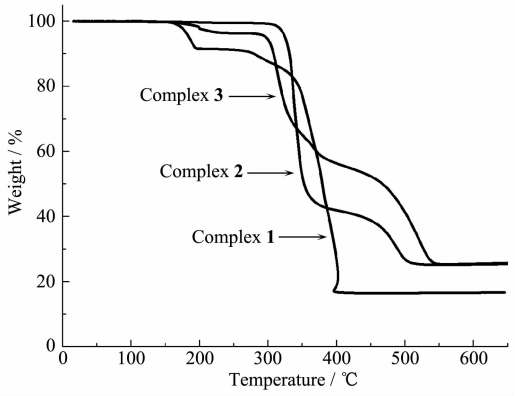

Fig.4 TGA curves for complexes **1**~**3**

2.3 Magnetic property

In the metal-carboxylate chain structure of complex **1**, the separation distance between two adjacent Ni(Ⅱ) ions is 0.533 83(5) nm, indicating that there are magnetic interactions exchanged by carboxylate bridges of the -CH_2COO^- groups along the chain. So the temperature-dependent magnetic susceptibility was measured at an applied magnetic field of 2 000 Oe from 2.5 to 300 K. And the curves of $\chi_M T$ vs T and χ_M vs T are shown in Fig.5. The observed $\chi_M T$ at 300 K was 1.05 $cm^3 \cdot K \cdot mol^{-1}$, which was near to the expected spin-only product of 1.00 $cm^3 \cdot mol^{-1} \cdot K$ for a uncoupled Ni(Ⅱ) ion. Upon cooling, it kept almost the same level in a wide temperature range of 76 to 300 K. Below 76 K, the $\chi_M T$ increased dramatically and reached to a maximum of 1.86 $cm^3 \cdot mol^{-1} \cdot K$ at 2.5 K. And similar change occurred in the curve of χ_M vs T. Because complex **1** can magnetically be handled as infinite uniform chains, the magnetic interaction (J) between two adjacent Ni(Ⅱ) ions can be estimated by using the classical spin expression derived from isotropic Heisenberg spin Hamiltonian chains[35-36]:

$$\hat{H}=-J\sum S_i S_{i+1},$$

$$\chi_M=[Ng^2\beta^2S(S+1)/3(kT)][(1+u)/(1-u)] \quad (1)$$

In Eq.(**1**), u is the Langevin function defined as $u=\coth[JS(S+1)/(kT)]-kT/[JS(S+1)]$ with S=1, while other parameters represent their usual meanings. The magnetic data of complex **1** fitted well with Eq.(**1**) in the whole temperature range. And the best fit led to fitting parameters as following: J=1.01 cm^{-1}, g=2.04 and $R=2.8\times10^{-4}$. Furthermore, these magnetic data obey the Curie-Weiss law $\chi_M=C/(T-\theta)$ from 2.5 to 300 K with Weiss constant θ=0.992 2 K, Curie constant C=1.044 3 $cm^3 \cdot K \cdot mol^{-1}$ and R=0.999 96. The positive J value and θ value, together with the increase of $\chi_M T$ value indicate that there are typical ferromagnetic exchange coupling between two adjacent Ni(Ⅱ) ions in uniform chain[37].

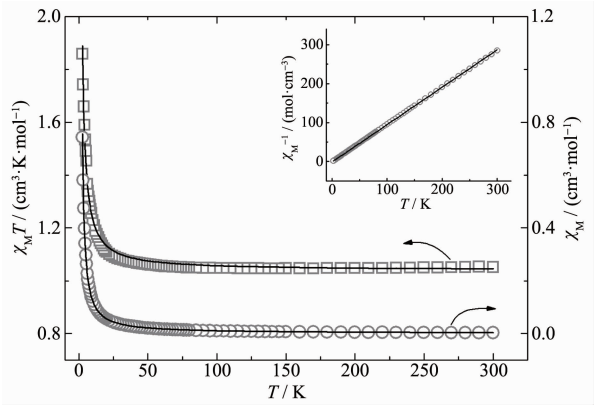

Inset: χ_M^{-1} vs T plot

Fig.5 Temperature dependences of magnetic susceptibility χ_M (○) and $\chi_M T$ (□) for complex **1**

2.4 Fluorescent properties

The fluorescent properties of complexes **2** and **3** in the solid state were investigated at room temperature, as illustrated in Fig.6. Under excitation at 305 nm, the maximum emission peak for complex **2** appeared at ~341 nm, and complex **3** exhibited the strongest peak at ~332 nm with excitation wavelength at 275 nm. For comparison, the fluorescent behaviors of H_2hmph, bib and bip ligands were detected. Featureless emissions with the maximum at ~452 nm (λ_{ex}=390 nm) for H_2hmph, ~385 nm (λ_{ex}=314 nm) for bib and ~418 nm (λ_{ex}=290 nm) for bip were observed, respectively. Taking account of the inherent properties of Cd/Zn metal centers and similar emission spectra shapes of the related complexes, the fluorescent properties of complexes **2** and **3** can probably be attributed to the ligand localized emission[38]. In comparison with the free organic precursors, obvious blue shifts of emission bands for **2** and **3** have been observed, which may be

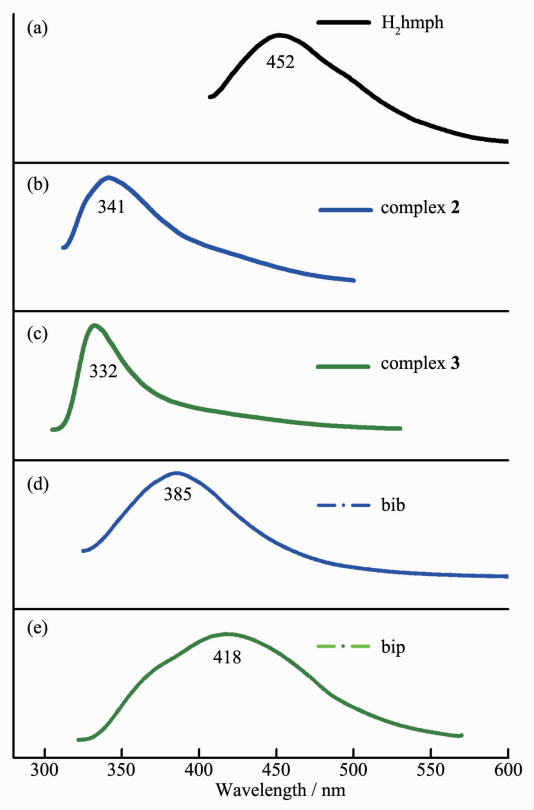

Fig.6　Solid-state emission spectra of complexes **2**~**3** and the related ligands at ambient temperature

attributed to the deprotonated effect of H_2hmph ligand, and the coordination interactions of the $hmph^{2-}$ and diimidazolyl-type ligands around the central metal ions[39].

3　Conclusions

Overall, treating Ni(Ⅱ)/Cd(Ⅱ)/Zn(Ⅱ) acetate with flexible homophthalic acid and diimidazolyl-type ligands yielded three novel coordination polymers under mild solvothermal routes. Complexes **1** and **2** possess 2D monolayer and bilayer structure featuring metal-carboxylate chains cross-linked by bib co-ligands, respectively. Complex **3** is double-stranded chain featuring Zn-carboxylate binuclear units extended by bip co-ligands. All three complexes have high thermal stabilities since their frameworks begin to collapse at 267 ℃ for **1**, 304 ℃ for **2** and 292 ℃ for **3**. In complex **1**, typical ferromagnetic exchange coupling exists between two adjacent Ni(Ⅱ) ions in uniform chain. Moreover, the solid state luminescence of complexes **2** and **3** is attributed to the ligand localized emission with significant blue-shift.

Supporting information is available at http://www.wjhxxb.cn

References:

[1] Moulton B, Zaworotko M J. *Chem. Rev.*, **2001**,**101**:1629-1658
[2] Zhu Q L, Xu Q. *Chem. Soc. Rev.*, **2014**,**43**:5468-5512
[3] Xuan W M, Zhu C F, Liu Y, et al. *Chem. Soc. Rev.*, **2012**, **41**:1677-1695
[4] Kumar G, Kumar G, Gupta R. *RSC Adv.*, **2016**,**6**:21352-21361
[5] Heine J, Müller-Buschbaum K. *Chem. Soc. Rev.*, **2013**,**42**: 9232-9242
[6] Das D, Biradha K. *Cryst. Growth Des.*, **2018**,**18**:3683-3692
[7] Tang Y W, Soares A C, Ferbinteanu M, et al. *Dalton Trans.*, **2018**,**47**:10071-10079
[8] Yin Z, Zhou Y L, Zeng M H, et al. *Dalton Trans.*, **2015**,**44**: 5258-5275
[9] XIAO Bo-An(肖伯安), CHEN Shui-Sheng(陈水生). *Chinese J. Inorg. Chem.*(无机化学学报), **2017**,**33**(2):347-353
[10]Miao S B, Li Z H, Xu C Y, et al. *CrystEngComm*, **2016**,**18**: 1625-1632
[11]Lin Z J, Lü J, Hong M C, Cao R. *Chem. Soc. Rev.*, **2014**,**43**: 5867-5895
[12]Pigge F C. *CrystEngComm*, **2011**,**13**:1733-1748
[13]Zhang Z Y, Xu L J, Cao R. *New J. Chem.*, **2018**,**42**:5593-5601
[14]Liu T F, Lü J, Cao R. *CrystEngComm*, **2010**,**12**:660-670
[15]Zhang X T, Chen H T, Li B, et al. *Dalton Trans.*, **2018**,**47**: 1202-1213
[16]WANG Yu-Fang(王玉芳), TAI Jun-Hui(太军慧), YAN Xiao-Wei(颜小伟), et al. *Chinese J. Inorg. Chem.*(无机化学学报), **2018**,**34**(6):1121-1126
[17]Li X L, Liu G Z, Xin L Y, et al. *J. Solid State Chem.*, **2017**, **246**:252-257
[18]Ju F Y, Li Y P, Li G L, et al. *Chin. J. Struct. Chem.*, **2016**, **35**:404-412
[19]Kang H X, Fu Y Q, Ju F Y, et al. *Russ. J. Coord. Chem.*, **2018**,**44**:340-346
[20]Xin L Y, Liu G Z, Ma L F, et al. *Inorg. Chim. Acta*, **2016**, **443**:64-68
[21]Li G L, Liu G Z, Ma L F, et al. *Chem. Commun.*, **2014**,**50**: 2615-2617
[22]Burrows A D, Harrington R W, Mahon M F, et al. *Eur. J. Inorg. Chem.*, **2003**:766-776
[23]Zhou J H, Wang Y, Wang S N, et al. *J. Coord. Chem.*, **2013**,

66:737-747

[24]Liu G Z, Xin L Y, Wang L Y. *CrystEngComm*, **2011**,**13**: 3013-3020

[25]Farnum G A, Wang C Y, Supkowski R M, et al. *Inorg. Chim. Acta*, **2011**,**375**:280-289

[26]Wang Y, Liu Z Q, Zhou J H, et al. *Inorg. Chim. Acta*, **2013**, **400**:169-178

[27]Orhan O, Colak A T, Sahin O, et al. *Polyhedron*, **2015**,**87**: 268-274

[28]Liu G Z, Zhang J, Wang L Y. *Polyhedron*, **2011**,**30**:1487-1493

[29]Rogers C M, Wang C Y, Farnum G A, et al. *Inorg. Chim. Acta*, **2013**,**403**:78-84

[30]Kraft P E, Uebler J W, Laduca R L. *J. Mol. Struct.*, **2013**, **1038**:86-94

[31]Burla M C, Caliandro R, Camalli M, et al. *J. Appl. Cryst.*, **2007**,**40**:609-613

[32]Dolomanov O V, Bourhis L J, Gildea R J, et al. *J. Appl. Cryst.*, **2009**,**42**:339-341

[33]Sheldrick G M. *Acta Crystallogr. Sect. C*: *Cryst. Struct. Commun.*, **2015**,**C71**:3-8

[34]Li Y P, Ju F Y, Li G L, et al. *Russ. J. Coord. Chem.*, **2018**, **44**:214-219

[35]Wang W B, Wang R Y, Liu L N, et al. *Cryst. Growth Des.*, **2018**,**18**:3449-3457

[36]Wang Y Q, Jia Q X, Wang K, et al. *Inorg. Chem.*, **2010**,**49**: 1551-1560

[37]Li G L, Yin W D, Liu G Z, et al. *J. Solid State Chem.*, **2014**,**220**:1-8

[38]QIAO Yu(乔宇), MA Bo-Nan(马博男), LI Xiu-Ying(李秀颖), et al. *Chinese J. Inorg. Chem.*(无机化学学报), **2015**,**31** (6):1245-1251

[39]Chang X H, Zhao Y, Feng X, et al. *Polyhedron*, **2014**,**83**: 159-166